A UNIVARIATE EXTREME VALUE ANALYSIS AND CHANGE POINT DETECTION OF MONTHLY DISCHARGE IN KALI KUPANG, CENTRAL JAVA, INDONESIA

THIS IS A **NON-PEER REVIEWED** PREPRINT SUBMITTED TO EARTHARXIV.SUBSEQUENT PEER-REVIEWED VERSIONS OF THIS MANUSCRIPT MAY HAVE SLIGHTLY DIFFERENT CONTENT. THE AUTHOR WELCOMES FEEDBACK.

Sandy H. S. Herho*
Department of Geology
University of Maryland
College Park, MD, USA 20742

May 18, 2022

ABSTRACT

This study presents how Extreme Value Analysis (EVA) can be used to predict future extreme hydrological events and how dynamic-programming based change point detection algorithm can be used to detect the abrupt transition in discharge events variability in Kali Kupang, Central Java, Indonesia. By using the annual block maxima, we can predict the upper extreme discharge probability from the Gumbel distribution, which is the extreme distribution that best fits the data, after distribution fitting using the Markov Chain Monte Carlo (MCMC) method. Using the pruned exact linear time (PELT) algorithm, with a change point location, it is known that the annual standard deviation of this time series has changed in the mid-1990s. Despite some shortcomings, this study can pave the way for the use of non-traditional data analysis algorithms in analyzing hydrological time-series data in the Indonesian region.

Keywords hydrological extreme · change point detection · block maxima · MCMC · PELT

1 Introduction

Kali Kupang, or locally known as Kali Loji, flows from the confluence of the Retno Sumilir tributaries located at the foothills of the Mount Rogojembangan – Petungkriyono, which is administratively located on the border of Banjarnegara and Pekalongan districts to its estuary, which is located in the Java Sea, north of the city of Pekalongan. Kali Kupang is also called the Masin river, because this river passes through a village called Masin, which is located in Warungasem, Batang district. This Masin village is referred to in classical Javanese Hindu history (1) as the Mo-Ho-Sin kingdom or the Mahasin kingdom. This kingdom was a Hindu kingdom in Java that developed in the 10th century AD. According to Ma-Huan, who was a secretary to Admiral Zheng He (2), the emergence of settlements in the Sampangan village area was the beginning of Pekalongan's development as an inter-island port and at that time, Kali Kupang was designated as its base. It is not known who is the ruler in this Pekalongan harbor area. At that time Pekalongan was still part of the vacant land of the Cirebon sultanate. In the Cirebon Kertabumi script by Wangsakerta in 1485, the Pekalongan area was once led by the Wu Hang family who was a great harbormaster who controlled trade traffic at the Pekalongan port. During the reign of the Islamic Mataram sultanate, around the 17th century AD, Pekalongan became a rich area. The large amount of money and abundant rice production that was sent to the center of the kingdom made Pekalongan an important part of the territory of the Mataram sultanate (2). Meanwhile, during the Dutch colonial period in the early 18th century AD until the 20th century AD, many merchant ships from various nations such as China, Arabia, India, and Europe docked at Kali Kupang until they passed the *Vereenigde Oostindische Compagnie* (VOC) guard post,

*herho@terpmail.umd.edu

namely Fort Peccalongan. This is evidenced by the many graves of sailors from various regions of the archipelago such as Bugis, Madura, Malay, and Kalimantan (1). The tombs of these sailors are located in the forest near Kali Kupang, to be precise in the Arab village of Suguhwaras (2). This was proven when Sayid Husein bin Salim, an Islamic scholar and trader from Hadramaut, built the Waqaf mosque in 1854 AD. Here many tombs are found with tombstones made of sea shells (2). Entering the era of 1830 after the Diponegoro war, when Pekalongan became a sugar-producing area for the Dutch kingdom, sugar exports to Europe also went through this Pekalongan port where Kali Kupang served as a transit point for Dutch trading ships before sailing back to Europe (2). In the era of the 18th to 20th century batik trade, many merchant ships entered the Loji area. The ship unloaded its cargo around Sugihwaras, because this area is a Batik market which is near Kali Kupang (2). Kali Kupang was also used as a berth for fishing boats until the early 1980s, before the Nusantara fisheries port was built in Pekalongan (2).

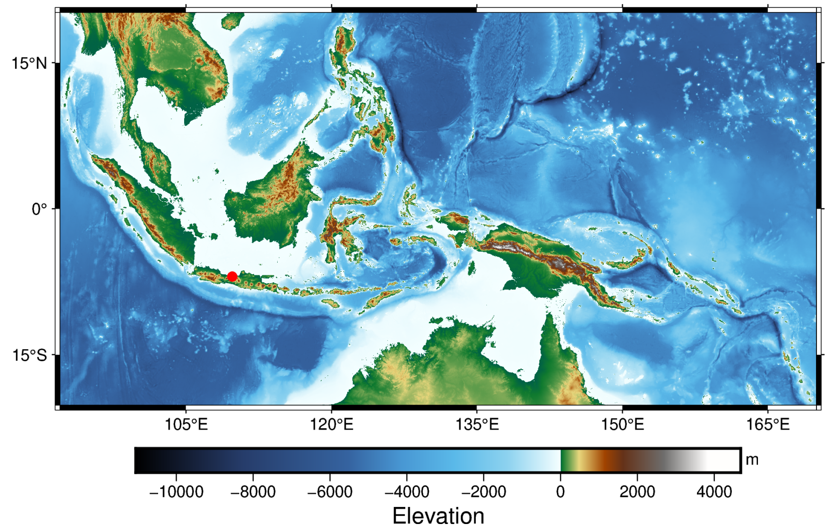

Figure 1: Map of the study region highlighting hydrological station in the region (red circle).

Due to the historical facts mentioned above, Kali Kupang plays a very important role in the lives of the people of Pekalongan and the surrounding area. In this study, I would like to examine the extremes and changes in the variability of the Kali Kupang flow. This study uses the average monthly discharge at Pagarukir station (7.03056°S, 109.76111°E) (Figure 1) with a time span of July 1975 to November 2009. These data were obtained from the Global Data Runoff Centre (GRDC) database (`https://www.bafg.de/GRDC/` accessed 17 May 2022) operated by GRDC at the German Federal Institute of Hydrology (BfG) in Koblenz, Germany.

2 Exploratory data analysis

Because there are 13.56% of missing data from the average monthly discharge time series, it is necessary to interpolate. This study uses a shape-preserving piecewise cubic hermite interpolation scheme (3) which is one of the interpolation methods that can smooth the curves at each data point (4). To simplify the numerical calculation process, I use the **pandas** library (5) in the Python computing environment to implement this interpolation scheme the missing data. The result of this interpolation is shown in Figure 2.

In order to discover the annual pattern of this time series, the data were averaged for each month throughout the time period. The result (Figure 3) is consistent with the precipitation study conducted by (6) which grouped Central Java into region A with one peak and one trough. This pattern is due to the strong influence of the northwest monsoon from November to March (NDJFM) and the southeast monsoon from May to September (MJJAS) (6).

To characterize the location and variability of these data, measurements of skewness and kurtosis. I use the Fisher-Pearson coefficient of sample skewness as follows,

$$g_1 = \frac{m_3}{m_2^{3/2}}. \tag{1}$$

Meanwhile, to measure the kurtosis of the sample, the following equation is used,

$$g_4 = \frac{m_4}{m_2} - 3 \tag{2}$$

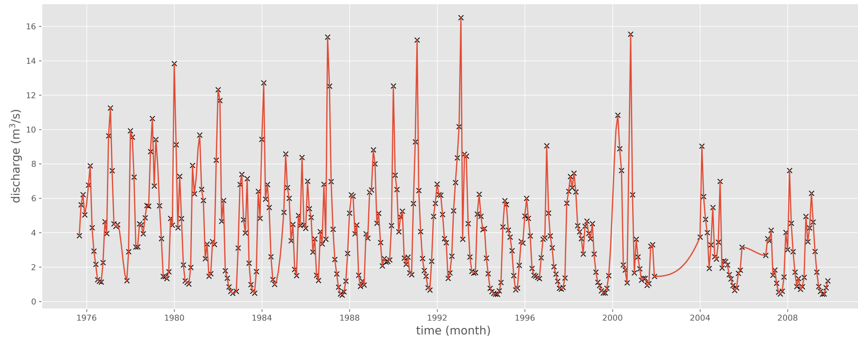

Figure 2: Shape-preserving piecewise cubic hermite interpolation of average monthly discharge (red line). Uninterpolated data points mark with x.

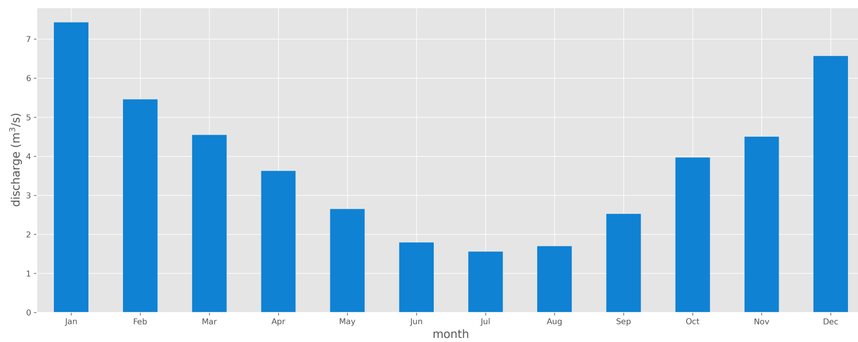

Figure 3: Annual cycle of average monthly discharge.

, where m_i is the moment coefficient defined as follows,

$$m_i = \frac{1}{N} \sum_{n=1}^{N} (x_n - \overline{x})^i. \tag{3}$$

In this study, the measurement of skewness and kurtosis is done automatically using the **scipy** library (7) in the Python computing environment. The values of skewness and kurtosis in this data are 1.313 and 2.146, respectively. This shows that the tail of this distribution is longer towards the right hand side of the curve ($g_1 > 0$) and is a flat distribution, where the values are moderately spread out or known as the platykurtic distribution ($g_4 < 3$). It appears from the results of this calculation, that these average monthly discharge data are not normal,which can also be seen in the distribution graph in Figure 4. However, to ensure that these data do not come from a normal distribution, a normality test must be carried out on these data. Due to relatively small number of samples, I use the Shapiro-Wilk test (8) on this data (9). Shapiro Wilks test is used to identify whether a random variable is normally distributed or not. This test is often applied in regression analysis to check the normality assumption of random error. The first step in the Shapiro-Wilk test is to determine the null hypothesis and the alternative hypothesis, namely:

- H_0: The population follows a normal distribution,
- H_1: The population does not follow a normal distribution.

Then, I determine the significance value of α, which in this case is 0.05. Then, the data are sorted from smallest to largest and divided into two groups for conversion in the Shapiro-Wilk test. Then, the statistical value of the Shapiro-Wilk test is calculated using the following equation,

$$T_3 = \frac{1}{D} \left[\sum_{i=1}^{n} a_i \left(x_{n-1+1} - x_i \right)^2 \right] \tag{4}$$

, where,

$$D = \sum_{i=1}^{n} (x_i - \overline{x})^2. \tag{5}$$

In this case, a_i is the Shapiro-Wilk test coefficient determined automatically, without using a table, using the **scipy** library (7) in the Python computing environment. The statistical value of the Shapiro-Wilk test is 0.886, with $p < 0.05$, so the null hypothesis can be rejected, therefore these data do not come from a Gaussian distribution.

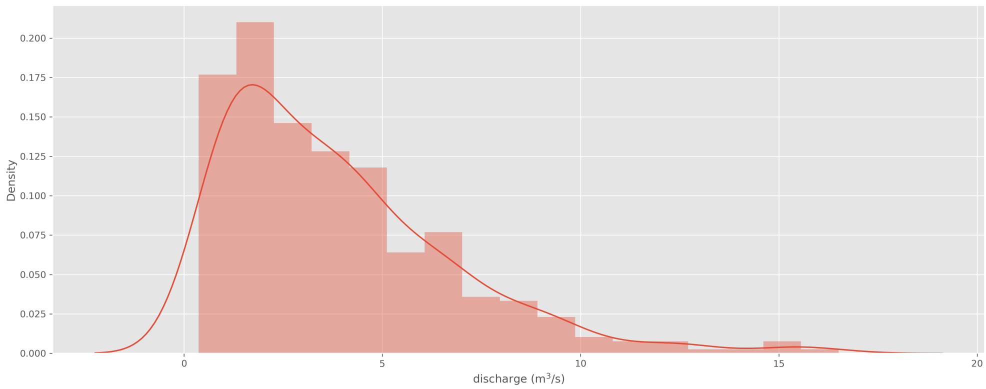

Figure 4: Distribution of average monthly discharge.

3 Extreme value analysis

Extreme events that often occur in the insurance, economic, climatology, hydrology, and telecommunications are indicated by the presence of a very high (maximum) and very low (minimum) observed value. The interesting thing is to determine the probability (maximum and minimum) of rare events (tail distribution). One of the statistical methods used to study the tail behavior of the distribution is extreme value analysis (EVA). EVA focuses on the behavior of the tail region of a distribution to be able to determine the probability of extreme values (10). An extreme value is derived from an event that occurs very rarely, is often declared an outlier and ignored but has a very large impact. The study of the distribution tail shows that in some cases the hydrological data has a heavy tail distribution (e.g., 11; 12; 13; 14; 15; 16), that is, the tail of the distribution decreases slowly when compared to the Gaussian distribution. According to the central limit theorem (CLT), the Gaussian distribution is the limit distribution of the sample mean. The Fisher-Tippet-Gnekendo theorem is analogous to the CLT and uses the tail index to unify the possible characterizations of the density function of the extreme value distribution (10). Coles (10) states that there are two methods for identifying extreme values, namely taking the maximum/minimum value in a certain period, which is often referred to as the block maxima/minima (BM) method and taking values that pass a threshold value, called the peaks over threshold (POT) method.In this analysis I use the annual block maxima approach (365.2425 days) on the data (Figure 5). This is done considering the ease and simplicity of this method compared to using POT. I purposely do not use block minima analysis, because of the possibility of constraints on the elevation limit of the riverbed elevation that required recalibration (17). Through this BM method, I can determine the generalized extreme value distribution (GEVD) that fits the data.

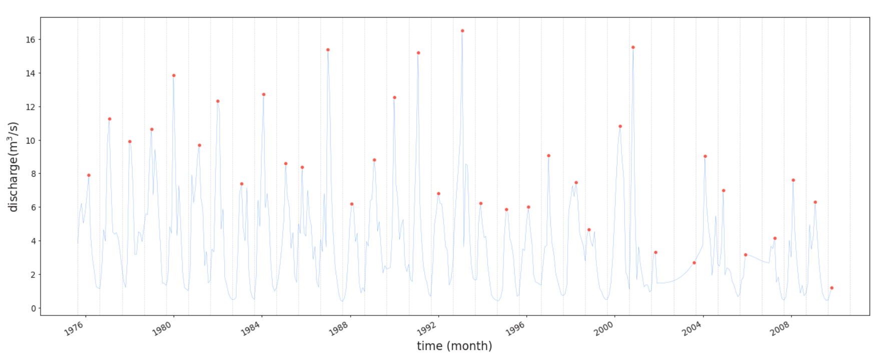

Figure 5: Annual block maxima of average monthly discharge.

The BM method is one of the EVA methods that can identify extreme values based on the highest value of observation data grouped by a certain period, which in this study is the value of average monthly discharge in a period of 365.2425 days (Figure 5). Samples of extreme values taken based on BM can be grouped as Gumbel, Fréchet, or Weibull distributions. The combination of these three distributions into one family is referred to as the GEVD distribution. The cumulative distribution function (CDF) of the GEVD is defined by the following equation,

$$F(x;\mu,\sigma,\xi) = \begin{cases} \exp\left\{-\left(1+\xi\left(\frac{x-\mu}{\sigma}\right)^{\frac{-1}{\xi}}\right)\right\}, & -\infty < x < +\infty, \quad \left(1+\xi\left(\frac{x-\mu}{\sigma}\right)\right) > 0 \\ \exp\left\{-\exp\left(-\frac{x-\mu}{\sigma}\right)\right\}, & -\infty < x < +\infty, \quad \xi = 0 \end{cases} \tag{6}$$

The GEVD is flexible in modeling different extreme behavior with three distribution parameters ($\boldsymbol{\theta} = (\mu, \sigma, \xi)$). The location parameter (μ), with $-\infty < \mu < +\infty$, is a parameter that determines the distribution center. The scale parameter (σ), with $\sigma > 0$, determines the size of the deviation around the location parameter. The shape parameter (ξ) governs the behavior of the GEVD tail. GEVD is divided into three types when viewed based on the value of the shape parameter (ξ), namely type I (Gumbel) if ξ = 0, type II (Fréchet) if $\xi > 0$, and type III (Weibull) if $\xi < 0$ (10).

Since the number of extreme values in the average monthly discharge data is relatively small, which only covers the maximum value for 35 years, so to stabilize the distribution fitting process, I use a Bayesian perspective (18), namely by using the Markov Chain Monte Carlo (MCMC) method which is considered more stable for determine the $\hat{\boldsymbol{\theta}} = (\hat{\mu}, \hat{\sigma}, \hat{\xi})$ parameters compared to the maximum likelihood estimation method which is commonly used for large samples (19).

MCMC is a method for generating random variables based on Markov chain (20). With MCMC, a correlated random sample sequence is obtained, i.e. the j^{th} value of the $\{\boldsymbol{\theta}_j\}$ sequence is sampled from a probability distribution that depends on the previous value of $\{\boldsymbol{\theta}_{j-1}\}$. The exact distribution of $\{\boldsymbol{\theta}_j\}$ is generally not known, but the distribution at each iteration in the sequence of sample values will converge to the true distribution for a sufficiently large value of j. Therefore, if the updated sample size is large enough then the last group of values sampled in the sequence, e.g. $\{\boldsymbol{\theta}_{P+1}, \boldsymbol{\theta}_{P+2}, \boldsymbol{\theta}_{P+3}, \cdots\}$ will approximate a sample originating from the desired GEVD (21). P is usually referred to as the burn in period.

There are two main algorithms used in MCMC, namely the Metropolis-Hastings algorithm and the Gibbs sampling algorithm. In this study, the Metropolis-Hasting (MH) algorithm is used to generate random samples from the desired posterior distribution (22). In the MH algorithm, a proposal distribution $p(\boldsymbol{\theta}|\boldsymbol{\theta}_{j-1})$ is needed to generate random sample candidates. The basic steps of this algorithm are as follows (21),

1. Take the initial value, which is $\boldsymbol{\theta}_0$ for iteration $j = 1$, generate $\boldsymbol{\theta}^* \sim p(\boldsymbol{\theta}|\boldsymbol{\theta}_{j-1})$.
2. Generate a random sample u from the uniform distribution $U[0, 1]$.
3. If $u <$ min $\left(1, \frac{p(\boldsymbol{\theta}^*|\boldsymbol{X},\boldsymbol{y})p(\boldsymbol{\theta}_{j-1}|\boldsymbol{\theta}^*)}{p(\boldsymbol{X},\boldsymbol{y}|\boldsymbol{\theta}^*)p(\boldsymbol{\theta}^*|\boldsymbol{\theta}_{j-1})}\right)$, then take $\boldsymbol{\theta}_j = \boldsymbol{\theta}^*$.

   But if $u >$ min $\left(1, \frac{p(\boldsymbol{\theta}^*|\boldsymbol{X},\boldsymbol{y})p(\boldsymbol{\theta}_{j-1}|\boldsymbol{\theta}^*)}{p(\boldsymbol{X},\boldsymbol{y}|\boldsymbol{\theta}^*)p(\boldsymbol{\theta}^*|\boldsymbol{\theta}_{j-1})}\right)$, then take $\boldsymbol{\theta}_j = \boldsymbol{\theta}_{j-1}$.
4. Repeat steps 1 to 3 up to the desired amount.

The statistic used to measure the degree of dependence between successive retrievals in a Markov chain is autocorrelation. Autocorrelation measures the correlation between two sets of simulated values $\{\boldsymbol{\theta}_j\}$ and $\{\boldsymbol{\theta}_{j+L}\}$, where L is the lag or number that separates the two sets. For a certain hyperparameter θ_i, the autocorrelation value in the L^{th} lag can be calculated by the following equation,

$$r_{iL} = \left(\frac{M}{M-L}\right)\left[\frac{\sum_{i=1}^{M-L}(\theta_i - \overline{\theta})(\theta_{i+L} - \overline{\theta})}{\sum_{i=1}^{M}(\theta_i - \overline{\theta})}\right] \tag{7}$$

, where M is the size of the random sample.

MCMC computing in this study uses the **emcee** library (23), which is a built-in from the **pyextremes** library (17) to perform GEVD fitting using the MCMC method. **Emcee** uses the ensemble samplers with affine invariance method to run the MH algorithm (23), which is proven to be significantly faster than the standard MH algorithm on highly skewed distributions (24). Therefore, there is the term walkers, which are the members of the ensemble. These walkers are like separate MH chains. In this study 500 walkers are used, with 2,500 samples for each walker. The MCMC trace and corner plots can be seen in Figure 6 as follows,

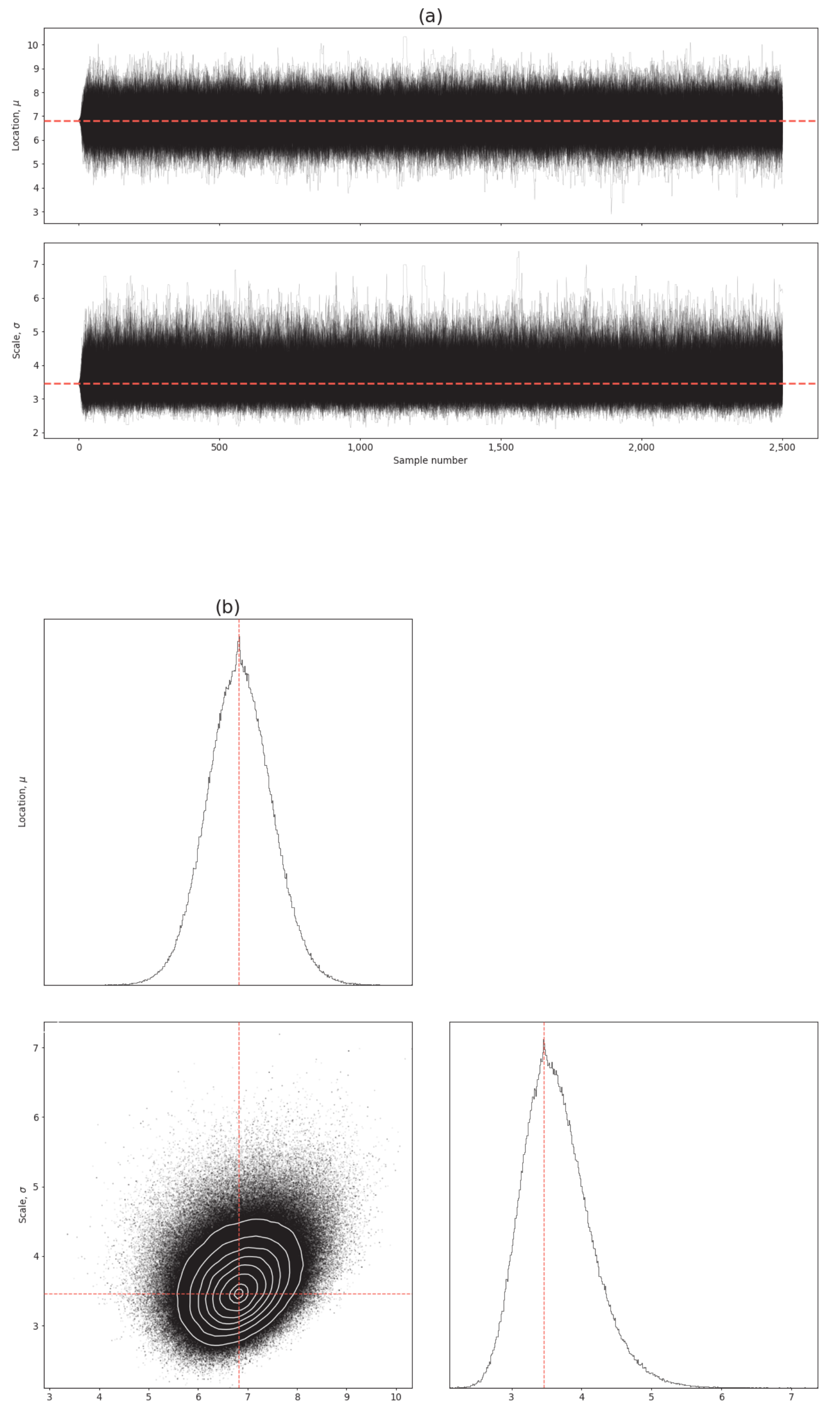

Figure 6: Annual block maxima parameter estimation using MCMC. (a) Trace plot for GEVD parameter estimation . The corner plot (b) shows all the one and two dimensional projections of the posterior probability distributions of GEVD parameters.

Through this MCMC computation, I get, parameter values $\hat{\mu} = 6.818$, $\hat{\sigma} = 3.456$, and $\hat{\xi} = 0$, so it can be concluded that the upper extreme value of this average monthly discharge can be classified into Gumbel distribution.

By using these GEVD parameters, recurrence intervals (RI) can be calculated from the upper extreme values for the annual average monthly discharge in Kali Kupang. RI is defined as the maximum value in the future period (10). RI in the context of this study is the maximum average monthly discharge that is expected to be exceeded once in a certain period of time. The maximum value is expected to be exceeded once in a period of k with period p, the average monthly discharge will reach the maximum value of R_k^p once. The estimated RI is expressed through the following equation,

$$\hat{R_k^p} = \begin{cases} \hat{\mu} - \frac{\hat{\sigma}}{\hat{\xi}} \left\{ 1 - \left(-\ln\left(1 - \frac{1}{k}\right) \right)^{-\hat{\xi}} \right\}, & \hat{\xi} \neq 0 \\ \hat{\mu} - \hat{\sigma} \ln\left\{ -\ln\left(1 - \frac{1}{k}\right) \right\}, & \hat{\xi} = 0. \end{cases} \tag{8}$$

The graphic visualization of this calculation is shown in Figure 7. The summary of RI can be seen in Table 1.

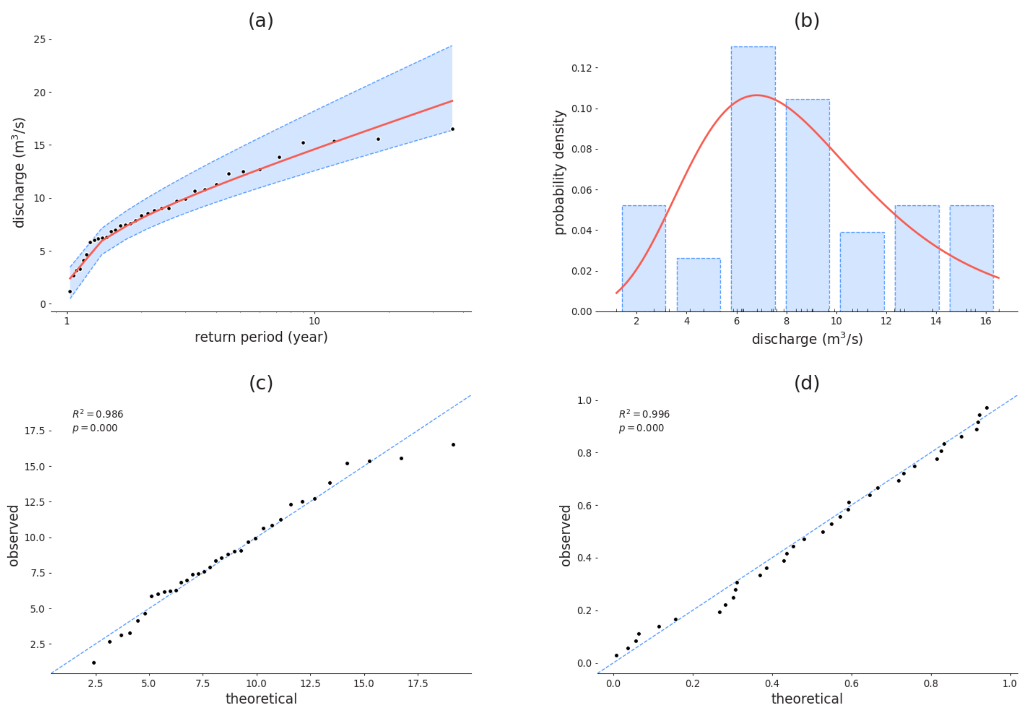

Figure 7: Diagnostic plots of average monthly discharge RI : (a) return level (shadded region corresponds to 95% confidence interval, (b) histogram with fitted GEVD density, (c) probability, (d) quantile.

Table 1: Average monthly discharge RI values.

Return Period (years)	Return Value (m^3/s)	Lower CI (m^3/s)	Upper CI (m^3/s)
2	8.0879	6.807	9.688
5	12.008	10.340	14.756
10	14.603	12.552	18.222
25	17.883	15.297	22.665
50	20.315	17.315	25.979
100	22.730	19.312	29.285

4 Change point detection

To determine the abrupt change in the average monthly discharge data, I use the pruned exact linear time (PELT) algorithm developed by Killick, *et. al.* (25). This algorithm has been widely used and is quite successful in detecting changes in the mean and variance of hydrological data in various regions (e.g., 26; 27; 28; 29; 30; 31). This algorithm is based on dynamic programming methods that are both fast and exact, nor does it rely on certain statistical assumptions. This algorithm works on a simple principle as follows,

$$\min_{\tau,k}\left[\sum_{j=0}^{k}\mathcal{C}\left(\boldsymbol{y}_{\tau_j+1:\tau_{j+1}}+\beta\right)\right] \tag{9}$$

, where $\boldsymbol{y}$ is the time series vector of the annual standard deviation of the average monthly discharge, $\mathcal{C}(.)$ is the cost function, β is the penalty term used to avoid overfitting, and τ is the vector of change point locations, which in this case I just use a single change point location in order to detect abrupt transition in the standard deviation. I use **ruptures** library (32) in in the Python computing environment to automate the calculation. A visual graph of this calculation is shown in Figure 8.

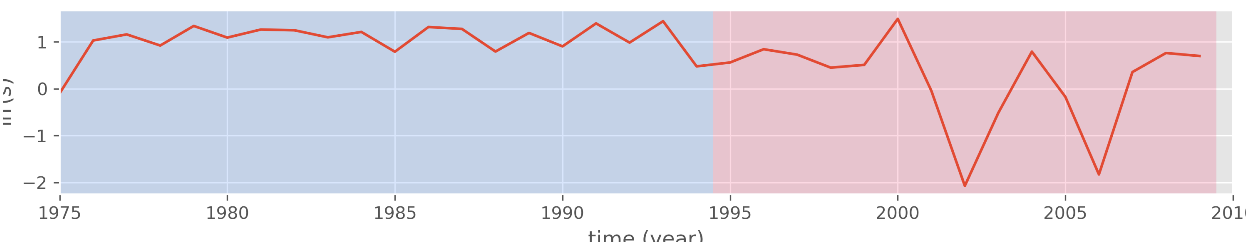

Figure 8: Change point detection with PELT algorithm. The y-axis is the annual standard deviation of the average monthly discharge in Kali Kupang displayed on a logarithmic scale.

It appears that there was a change in discharge variability after the mid-1990s. This change may have occurred because manufacturing-based development began to be encouraged at the end of the New Order era in the 1990s (33). With the increase in the manufacturing industry (34), it is possible to trigger population density in the area around the Kali Kupang watershed which causes various causes of changes in discharge variability (35; 36; 37). However, this can also be caused by the artifacts of filling in missing data that often occurred in the 2000s, so further analysis is needed in this section.

5 Concluding remarks and future work suggestion

In this study, univariate EVA and PELT change point detection are carried out on average monthy discharge data in Kali Kupang. The computational results of EVA using a Bayesian perspective succeeded in showing the RI values drawn from the Gumbel distribution. This may be used as a basis for decision-making for regional governments that are traversed by the Kali Kupang watershed, namely Banjarnegara regency, Batang regency, Pekalongan city, and Pekalongan regency to implement related infrastructure planning (e.g., 38; 39; 40). The computational results of change point detection using the PELT algorithm are able to detect abrupt shifts in the annual standard deviation from the average monthly discharge in the mid-1990s, to be precise in 1995.

However, this study has many shortcomings that need to be corrected. The main thing to do is to collect data on other stations, which unfortunately cannot be found on the GRDC database. This must be done because the Kali Kupang watershed is quite wide with an area of 18,022.193 ha. However, if there is no data for any station, it may be possible to simulate discharge using a numerical model, such as HEC HMS (e.g., 41; 42; 43; 44). In addition to that, there are other problems because there is no data from other stations in the same watershed, it is not possible to use double-mass curves (45), which are popularly used by hydrologists to replace the missing data. I have to interpolate missing data. This interpolation process is prone to cause time series artifacts, so further analysis of missing data imputation is required (e.g., 46; 47; 48). Furthermore, discharge data, like other hydroclimatological data (49), generally are not stationary, therefore adjustments are needed using non-stationary EVA (50). Unfortunately, pyextremes does not yet have this feature, so it is necessary to rewrite the code or switch to the **extRemes** package (19) in the R computing environment which already has the capability to perform non-stationary EVA. Improvements in this study need to be made considering the vitality of Kali Kupang for the lives of the people of Pekalongan and the surrounding areas. The potential use of data-driven computational methods (51) in this study can be further developed to anticipate extreme hydrological disasters that are likely to occur more in the future (52).

Code and data availability

Data are available through the cited sources throughout the article. Python scripts used in this study are accesible at `https://github.com/sandyherho/kaliKupangDisch`.

Competing interest

The author declares that I have no known competing financial interests or personal relationships that could have appeared to influence the work reported in this paper.

Acknowledgements

Amanda O'Shaughnessy, Cullen Simon, Gisma Firdaus, Karen Prestegaard, Joseph Malin, Julianne Farnham, Samantha Volz, and Sydney Shelton are acknowledged for providing valuable discussion. This study was supported by NSF grant AGS1903626.

References

[1] R. N. Poerbatjaraka, *Riwayat Indonesia Djilid I*. Jakarta: Yayasan Pembangunan, 1952.

[2] M. Dirhamsyah, *Pekalongan Yang (Tak) Terlupakan*. Pekalongan: KPAD Kota Pekalongan, 2015.

[3] F. N. Fritsch and R. E. Carlson, "Monotone piecewise cubic interpolation," *SIAM Journal on Numerical Analysis*, vol. 17, no. 2, pp. 238–246, 1980.

[4] C. B. Moler, *Numerical computing with MATLAB*. Society for Industrial and Applied Mathematics, 2011.

[5] W. McKinney, "Data Structures for Statistical Computing in Python," in *Proceedings of the 9th Python in Science Conference* (S. van der Walt and J. Millman, eds.), pp. 56 – 61, 2010.

[6] E. Aldrian and R. D. Susanto, "Identification of three dominant rainfall regions within indonesia and their relationship to sea surface temperature," *International Journal of Climatology*, vol. 23, no. 12, pp. 1435–1452, 2003.

[7] P. Virtanen, R. Gommers, T. E. Oliphant, M. Haberland, T. Reddy, D. Cournapeau, E. Burovski, P. Peterson, W. Weckesser, J. Bright, S. J. van der Walt, M. Brett, J. Wilson, K. J. Millman, N. Mayorov, A. R. J. Nelson, E. Jones, R. Kern, E. Larson, C. J. Carey, İ. Polat, Y. Feng, E. W. Moore, J. VanderPlas, D. Laxalde, J. Perktold, R. Cimrman, I. Henriksen, E. A. Quintero, C. R. Harris, A. M. Archibald, A. H. Ribeiro, F. Pedregosa, P. van Mulbregt, and SciPy 1.0 Contributors, "SciPy 1.0: Fundamental Algorithms for Scientific Computing in Python," *Nature Methods*, vol. 17, pp. 261–272, 2020.

[8] S. S. Shapiro and M. B. Wilk, "An analysis of variance test for normality (complete samples)," *Biometrika*, vol. 52, no. 3/4, pp. 591–611, 1965.

[9] A. Ghasemi and S. Zahediasl, "Normality tests for statistical analysis: a guide for non-statisticians," *International journal of endocrinology and metabolism*, vol. 10, no. 2, p. 486, 2012.

[10] S. Coles, *An Introduction to Statistical Modeling of Extreme Values*. London: Springer London, 2001.

[11] I. Ologhadien, "Study of unbiased plotting position formulae for the generalized extreme value (gev) distribution," *European Journal of Engineering and Technology Research*, vol. 6, no. 4, pp. 94–99, 2021.

[12] J. Sampaio and V. Costa, "Bayesian regional flood frequency analysis with gev hierarchical models under spatial dependency structures," *Hydrological Sciences Journal*, vol. 66, no. 3, pp. 422–433, 2021.

[13] H. Tabari, "Extreme value analysis dilemma for climate change impact assessment on global flood and extreme precipitation," *Journal of Hydrology*, vol. 593, p. 125932, 2021.

[14] E. Towler, D. Llewellyn, A. Prein, and E. Gilleland, "Extreme-value analysis for the characterization of extremes in water resources: A generalized workflow and case study on new mexico monsoon precipitation," *Weather and Climate Extremes*, vol. 29, p. 100260, 2020.

[15] F. De Paola, M. Giugni, F. Pugliese, A. Annis, and F. Nardi, "Gev parameter estimation and stationary vs. non-stationary analysis of extreme rainfall in african test cities," *Hydrology*, vol. 5, no. 2, 2018.

[16] Y. Liu, Y. Hao, Y. Fan, T. Wang, X. Huo, Y. Liu, and T.-C. J. Yeh, "A nonstationary extreme value distribution for analysing the cessation of karst spring discharge," *Hydrological Processes*, vol. 28, no. 20, pp. 5251–5258, 2014.

[17] G. Bocharov, "pyextremes."

[18] I. Jeliazkov and E. Lee, "Mcmc perspectives on simulated likelihood estimation," *Advances in Econometrics*, vol. 26, pp. 3–39, 12 2010.

[19] E. Gilleland and R. W. Katz, "extremes 2.0: An extreme value analysis package in r," *Journal of Statistical Software*, vol. 72, no. 8, p. 1–39, 2016.

[20] G. Casella and R. L. Berger, *Statistical inference*. Belmont, CA: Cengage Learning, 2021.

[21] D. Gamerman and H. F. Lopes, *Markov chain Monte Carlo: stochastic simulation for Bayesian inference*. Boca Raton, FL: CRC press, 2006.

[22] W. K. Hastings, "Monte Carlo sampling methods using Markov chains and their applications," *Biometrika*, vol. 57, pp. 97–109, 04 1970.

[23] D. Foreman-Mackey, D. W. Hogg, D. Lang, and J. Goodman, "ttemcee/tt: The MCMC hammer," *Publications of the Astronomical Society of the Pacific*, vol. 125, pp. 306–312, mar 2013.

[24] J. Goodman and J. Weare, "Ensemble samplers with affine invariance," *Communications in applied mathematics and computational science*, vol. 5, no. 1, pp. 65–80, 2010.

[25] R. Killick, P. Fearnhead, and I. A. Eckley, "Optimal detection of changepoints with a linear computational cost," *Journal of the American Statistical Association*, vol. 107, no. 500, pp. 1590–1598, 2012.

[26] D. T. Myers, D. L. Ficklin, S. M. Robeson, R. P. Neupane, A. Botero-Acosta, and P. M. Avellaneda, "Choosing an arbitrary calibration period for hydrologic models: How much does it influence water balance simulations?," *Hydrological Processes*, vol. 35, no. 2, p. e14045, 2021.

[27] N. Singh and P. Chinnasamy, "Non-stationary flood frequency analysis and attribution of streamflow series: a case study of periyar river, india," *Hydrological Sciences Journal*, vol. 66, no. 13, pp. 1866–1881, 2021.

[28] R. V. Rocha and F. A. S. Filho, "Mapping abrupt streamflow shift in an abrupt climate shift through multiple change point methodologies: Brazil case study," *Hydrological Sciences Journal*, vol. 65, no. 16, pp. 2783–2796, 2020.

[29] "Change points in annual peak streamflows: Method comparisons and historical change points in the united states," *Journal of Hydrology*, vol. 583, p. 124307, 2020.

[30] M. Sakizadeh and L. Chua, "Environmental impact of karkheh dam in the southern part of iran on groundwater quality by intervention and trend analysis," *Environmental Monitoring and Assessment*, vol. 192, no. 683, 2020.

[31] P. Gogumalla, S. Dubey, S. Tripathi, and D. Chandniha, "Trend and change point detection of precipitation in urbanizing districts of uttarakhand in india," *Indian Journal of Science and Technology*, vol. 7, pp. 1573–1582, 10 2014.

[32] C. Truong, L. Oudre, and N. Vayatis, "Selective review of offline change point detection methods," *Signal Processing*, vol. 167, p. 107299, 2020.

[33] B. Masitho, "Dinamika politik pembangunan pada masa orde baru (studi tentang industrialisasi ketergantungan dan peran modal jepang)," *PERSPEKTIF*, vol. 3, no. 2, 2014.

[34] R. Thombs and A. Jorgenson, "Manufacturing the urban rift: A cross-national study of urbanization, manufacturing, and co2 emissions, 2000-2013," *Human Ecology Review*, vol. 25, 12 2019.

[35] D. Pumo, E. Arnone, A. Francipane, D. Caracciolo, and L. Noto, "Potential implications of climate change and urbanization on watershed hydrology," *Journal of Hydrology*, vol. 554, pp. 80–99, 2017.

[36] E.-S. Chung, K. Park, and K. S. Lee, "The relative impacts of climate change and urbanization on the hydrological response of a korean urban watershed," *Hydrological Processes*, vol. 25, no. 4, pp. 544–560, 2011.

[37] J. Sheng and J. P. Wilson, "Watershed urbanization and changing flood behavior across the los angeles metropolitan region," *Natural Hazards*, vol. 48, no. 1, pp. 41–57, 2009.

[38] P. E. Kindermann, W. S. Brouwer, A. van Hamel, M. van Haren, R. P. Verboeket, G. F. Nane, H. Lakhe, R. Prajapati, and J. C. Davids, "Return level analysis of the hanumante river using structured expert judgment: A reconstruction of historical water levels," *Water*, vol. 12, no. 11, p. 3229, 2020.

[39] M. Bashirgonbad, N. A. Moghaddam, S. S. Khalighi, M. Mahdavi, E. Paque, and M. Lang, "Comparative study of frequency analysis and hydro-climatic methods for estimating maximum flood discharge (case study: Bakhtiary watershed)," 2018.

[40] F. E. Eregno, V. Nilsen, R. Seidu, and A. Heistad, "Evaluating the trend and extreme values of faecal indicator organisms in a raw water source: a potential approach for watershed management and optimizing water treatment practice," *Environmental Processes*, vol. 1, no. 3, pp. 287–309, 2014.

[41] C. Kabeja, R. Li, J. Guo, D. E. R. Rwatangabo, M. Manyifika, Z. Gao, Y. Wang, and Y. Zhang, "The impact of reforestation induced land cover change (1990–2017) on flood peak discharge using hec-hms hydrological model and satellite observations: a study in two mountain basins, china," *Water*, vol. 12, no. 5, p. 1347, 2020.

[42] A. Sarminingsih, A. Rezagama, *et al.*, "Simulation of rainfall-runoff process using hec-hms model for garang watershed, semarang, indonesia," in *Journal of Physics: Conference Series*, vol. 1217, p. 012134, IOP Publishing, 2019.

[43] A. Saleh, R. Ghobad, and R. Noredin, "Evaluation of hec-hms methods in surface runoff simulation (case study: Kan watershed, iran)," *Advances in Environmental Biology*, pp. 1316–1322, 2011.

[44] X. Chu and A. Steinman, "Event and continuous hydrologic modeling with hec-hms," *Journal of Irrigation and Drainage Engineering*, vol. 135, no. 1, pp. 119–124, 2009.

[45] J. Searcy and C. Hardison, "Double-mass curves. manual of hydrology—part 1—general surfacewater techniques, methods and practices of the geological survey," *US Geological Survey water-supply paper. Waterlow and Sons*, 1962.

[46] M. R. Zaghiyan, S. Eslamian, A. Gohari, and M. S. Ebrahimi, "Temporal correction of irregular observed intervals of groundwater level series using interpolation techniques," *Theoretical and Applied Climatology*, vol. 145, no. 3, pp. 1027–1037, 2021.

[47] E. L. Dan, M. Dînşoreanu, and R. C. Mureşan, "Accuracy of six interpolation methods applied on pupil diameter data," in *2020 IEEE International Conference on Automation, Quality and Testing, Robotics (AQTR)*, pp. 1–5, IEEE, 2020.

[48] I. Azizan, S. A. B. A. Karim, and S. S. K. Raju, "Fitting rainfall data by using cubic spline interpolation," in *MATEC Web of Conferences*, vol. 225, p. 05001, EDP Sciences, 2018.

[49] R. T. Clarke, "Hydrological prediction in a non-stationary world," *Hydrology and Earth System Sciences*, vol. 11, no. 1, pp. 408–414, 2007.

[50] L. Cheng, A. AghaKouchak, E. Gilleland, and R. W. Katz, "Non-stationary extreme value analysis in a changing climate," *Climatic change*, vol. 127, no. 2, pp. 353–369, 2014.

[51] D. P. Solomatine, "Data-driven modelling: paradigm, methods, experiences," in *Proc. 5th international conference on hydroinformatics*, pp. 1–5, 2002.

[52] P. R. Shukla, J. Skeg, E. C. Buendia, V. Masson-Delmotte, H.-O. Pörtner, D. Roberts, P. Zhai, R. Slade, S. Connors, S. van Diemen, *et al.*, "Climate change and land: an ipcc special report on climate change, desertification, land degradation, sustainable land management, food security, and greenhouse gas fluxes in terrestrial ecosystems," 2019.